Stray Capacitances of Single-Layer Solenoid Air-Core Inductors

Gabriele Grandi, Marian K. Kazimierczuk, *Senior Member, IEEE*, Antonio Massarini, and Ugo Reggiani, *Member, IEEE*

***Abstract*—This paper presents a method for predicting parasitic capacitances of solenoid HF inductors made of one layer of turns with circular cross sections, uniformly wound around a cylindrical nonconductive core. The method is based on an analytical approach to obtain the turn-to-turn and turn-to-shield capacitances of coils. The influence of the wire insulation is taken into account. An equivalent lumped parallel capacitance is derived. The method was tested by experimental measurements. The calculated and measured values were in good agreement in the considered cases. The derived expressions are useful for designing HF inductors and can also be adopted for modeling and simulation purposes.**

***Index Terms*—Equivalent circuits, HF inductors, stray capacitances.**

I. Introduction

THE behavior of air-core inductors at high frequencies is very different from that at low frequencies. Skin and proximity effects cause the winding resistance to increase as approximately $\sqrt{f}$ and the inductance to decrease slightly with increasing operating frequency f. Furthermore, the parasitic capacitances of the winding cannot be neglected at high frequencies. Parasitic capacitances significantly affect the inductor behavior and are responsible for resonant frequencies. An inductor behaves like a capacitor above its first (parallel) self-resonant frequency. Inductors used in EMC filters, RF power amplifiers, and radio transmitters operate at frequencies above several hundred kilohertz. Therefore, for an accurate prediction of the response of these inductors, the calculation of stray capacitances may be crucial for the design. Since the parasitic capacitances are distributed parameters, predicting the frequency response of an inductor is a difficult task. The high-frequency behavior of wound components is widely discussed in the literature, but mainly the aspects related to the parasitic ac resistance of the winding have been addressed [1]–[3].

Paper IPCSD 99–40, presented at the 1996 Industry Applications Society Annual Meeting, San Diego, CA, October 6–10, and approved for publication in the IEEE TRANSACTIONS ON INDUSTRY APPLICATIONS by the Power Electronics Devices and Components Committee of the IEEE Industry Applications Society. Manuscript released for publication March 18, 1999.

G. Grandi and U. Reggiani are with the Department of Electrical Engineering, University of Bologna, 40136 Bologna, Italy (e-mail: gabriele.grandi@mail.ing.unibo.it; ugo.reggiani@mail.ing.unibo.it).

M. K. Kazimierczuk is with the Department of Electrical Engineering, Wright State University, Dayton, OH 45435 USA (e-mail: mkazim@valhalla.cs.wright.edu).

A. Massarini is with the Department of Engineering Sciences, University of Modena and Reggio Emilia, 41100 Modena, Italy (e-mail: antonio.massarini@mail.ing.unibo.it).

Publisher Item Identifier S 0093-9994(99)06506-8.

Some results concerning stray capacitances of single-layer and multiple-layer coils are presented in [4]–[10]. These publications offer some interesting physical insights, but the results rely on experimental data. A novel simplified method for evaluating the stray capacitances of inductors is presented in [11] and [12]. This method is suited for inductors made of a conductive ferromagnetic core and multiple-layer windings consisting of layers of turns that are close to one another. Yet, the method is not sufficiently accurate when the inductor consists of only one layer of turns and a nonconductive core and the distance between turns is increased.

The purpose of this paper is to present a method for calculating stray capacitances of single-layer solenoid air-core inductors using an analytical approach based on few simplifying assumptions. The presence of a shield surrounding the inductor is taken into account. The proposed method can predict the overall stray capacitance of an inductor as a function of its geometry.

II. Proposed Method

A. Inductor Models

In EMC filtering applications, the frequencies of interest can range up to tens of megahertz. In order to minimize the effects of parasitic capacitances, inductors are usually made of a single wire wound as a single-layer solenoid, and the use of a conductive ferromagnetic core should be avoided. Hence, these inductors have neither turn-to-turn capacitances between turns of different layers nor turn-to-core capacitances. Furthermore, an air core does not suffer from hysteresis and eddy-current losses. The distance between turns is usually increased enough to reduce turn-to-turn capacitances. Inductors for EMC applications, such as those used in line impedance stabilizing networks (LISN's), are usually surrounded by an external shield. The presence of an external shield can give some contribution to the overall stray capacitance of such inductors.

A detailed HF equivalent circuit for a single-layer solenoid air-core inductor with a shield is shown in Fig. 1. Its parameters are related to every turn or pair of turns of the winding. The stray capacitances of the single-layer air-core n-turn inductor depicted in Fig. 1 are as follows:

- turn-to-turn capacitances $C_{t(i,\,j)}, i, j = 1, 2, \cdots, n; i \neq j;$
- turn-to-shield capacitances $C_{si},\ i = 1, 2, \cdots, n.$

In Fig. 1, R_i and L_i are the winding resistance and the self-inductance of the ith turn, respectively, and $M_{i,\,i+1}$ and $M_{i,\,i+2}$ represent the mutual inductances between pairs of

0093–9994/99$10.00 © 1999 IEEE

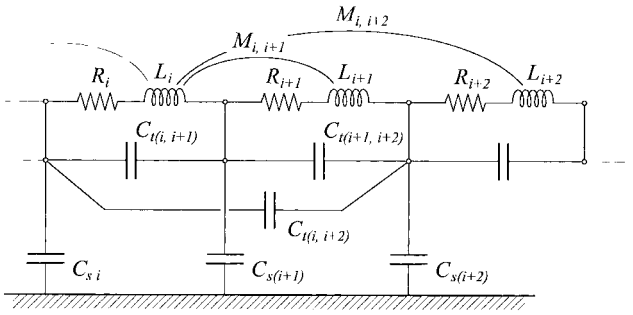

Fig. 1. HF equivalent circuit of single-layer solenoid air-core inductors with a shield.

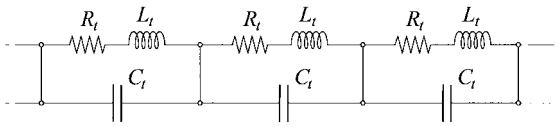

Fig. 2. HF equivalent circuit of single-layer solenoid air-core inductors without a shield and neglecting fringe effects.

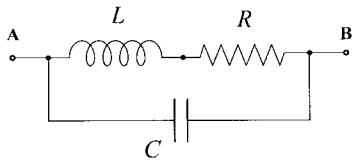

Fig. 3. Simplified HF equivalent circuit of single-layer solenoid air-core inductors without a shield.

turns. Because of symmetries of the winding,

$$C_{t(i,\,i+1)} = C_{t(i+1,\,i+2)} = \cdots = C_{tt}$$
$$C_{si} = C_{s(i+1)} = \cdots = C_{ts}$$
$$R_i = R_{i+1} = \cdots = R_t = R/n$$

where R is the total coil resistance.

If a uniform voltage distribution along the winding can be assumed, we can reduce the circuit shown in Fig. 1 to the simpler model depicted in Fig. 2. The condition of uniform voltage distribution is satisfied when there is no shield (or the influence of the shield can be neglected) and fringe effects are negligible. The simplifications introduced are justified by symmetry considerations which imply that inductive and capacitive effects are the same for all turns and, therefore, the same current flows through all turns. In particular, each turn has the same series equivalent self-inductance $L_t = L/n$, where L is the overall coil inductance. The capacitance C_t in Fig. 2 represents the equivalent capacitance between two corresponding points of any pair of adjacent turns. It consists of turn-to-turn capacitances between both adjacent and nonadjacent turns.

From the equivalent circuit of Fig. 2, we can obtain the simplified HF model of inductors without shield shown in Fig. 3, the parameters of which satisfy the following relations:

$$L = nL_t \quad R = nR_t \quad C = \frac{C_t}{n-1}. \tag{1}$$

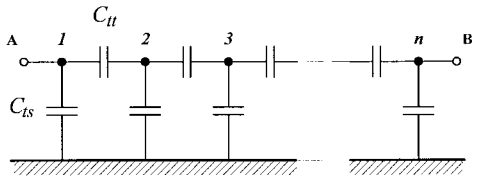

Fig. 4. Model of single-layer solenoid air-core inductors with a shield above the first self-resonant frequency.

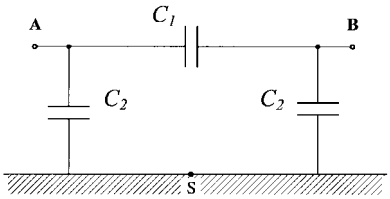

Fig. 5. Equivalent π-circuit of single-layer solenoid air-core inductors with a noninsulated shield above the first self-resonant frequency.

Above the first self-resonant frequency, the impedances of the *RLM* branches of the equivalent circuit of Fig. 1 become much higher than those of the shunt capacitances between adjacent turns. We can also assume that capacitances between nonadjacent turns can be neglected, because they are usually much smaller than capacitances between adjacent turns. In Section III, the relative error due to this assumption and its dependence on the geometrical dimensions of the inductors are highlighted. As a consequence, the equivalent circuit of Fig. 1 simplifies to the form in Fig. 4 [13]. In this case, the turn-to-shield capacitances (if they can considerably affect the overall impedance in this frequency range) can be taken into account and, consequently, the voltage along the winding is distributed according to the law of hyperbolic functions [13]. If the shield is not insulated, it may be important to consider also the partial capacitances C_2 between each terminal and the shield, in addition to the partial capacitance C_1 between terminals, thus introducing the equivalent π-circuit of Fig. 5. The capacitances C_1 and C_2 depend on both turn-to-turn and turn-to-shield capacitances, as will be shown in the next section.

B. Calculation of the Overall Stray Capacitance

For the circuit shown in Fig. 3, the overall stray capacitance C is given by (1). The equivalent turn capacitance C_t can be calculated neglecting the contribution of nonadjacent turns, so that C_t is reduced to the capacitance C_{tt} between two adjacent turns.

In order to evaluate the overall stray capacitance C_{AB} of the circuit depicted in Fig. 4, the conducting shield can be regarded as a single node, at which all the turn-to-shield capacitances C_{ts} are connected, and the symmetries of the circuit can be exploited. For a coil with an even number of turns, we firstly can consider the two turns in the middle of the winding. For these two turns, the capacitive network consists of the capacitance between the two turns in parallel with the series combination of the turn-to-shield capacitances.

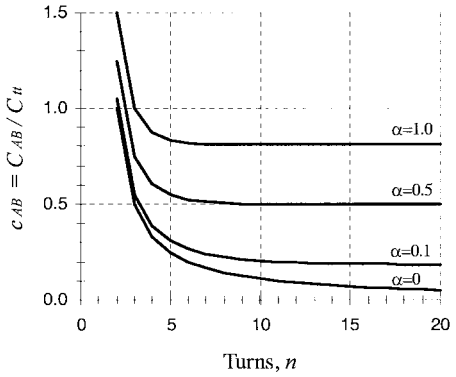

Fig. 6. Normalized overall capacitance for various values of the ratio $\alpha = C_{ts}/C_{tt}$.

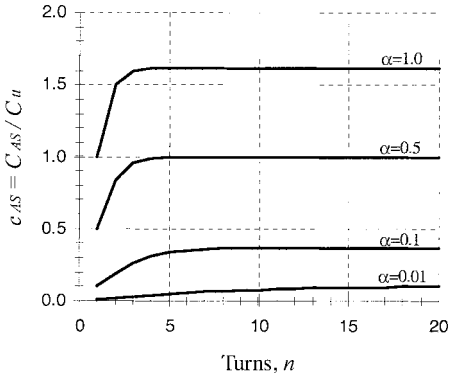

Fig. 7. Normalized capacitance between a coil terminal and the shield for various values of the ratio $\alpha = C_{ts}/C_{tt}$.

The equivalent capacitance of this network is

$$C_{AB}(2) = C_{tt} + \frac{C_{ts}}{2}. \tag{2}$$

For coils consisting of an odd number of turns, we first consider the three turns placed in the middle of the winding. The equivalent capacitance of the network associated with these three turns is given by

$$C_{AB}(3) = \frac{C_{tt}}{2} + \frac{C_{ts}}{2}. \tag{3}$$

In order to find the overall capacitance for coils consisting of larger numbers of turns, we can start from the two-turns (or three-turns) network and add systematically one more turn at each side of the network, the equivalent capacitance of which has been already obtained. The added turns introduce two more turn-to-turn and turn-to-shield capacitances. The equivalent capacitance of the previous network results in being in series with two more turn-to-turn capacitances and then in parallel with the series combination of two more turn-to-shield capacitances. Thus, for the network with a larger number of turns, we obtain the total stray capacitance

$$C_{AB}(n) = \frac{C_{AB}(n-2)\cdot C_{tt}/2}{C_{AB}(n-2) + C_{tt}/2} + \frac{C_{ts}}{2}, \qquad \text{for } n > 3. \tag{4}$$

Normalizing C_{AB} with respect to C_{tt} and introducing the capacitance ratio $\alpha = C_{ts}/C_{tt}$, (4) becomes

$$c_{AB}(n) = \frac{C_{AB}(n)}{C_{tt}} = \frac{1}{2 + C_{tt}/C_{AB}(n-2)} + \frac{\alpha}{2}. \tag{5}$$

Starting from (2) and (3), and using (4) or (5), we can calculate the overall capacitances of coils made of either an even or an odd number of turns, respectively. Furthermore, for large values of n, (5) converges to a finite limit, as shown in Fig. 6. It can be seen that the convergence is faster for higher values of α.

We found that the convergence limit of c_{AB} for $n \to \infty$ in terms of α is given by the following expression:

$$c_{AB}(\infty) = \frac{C_{AB}(\infty)}{C_{tt}} = \frac{1}{4}\,(\alpha + \sqrt{\alpha^2 + 4\alpha}). \tag{6}$$

For the model of Fig. 5, in order to calculate the partial capacitances C_1 and C_2, it is necessary to determine also the equivalent capacitance between each of the two coil terminals and the shield (e.g., C_{AS}, and $C_{BS} = C_{AS}$). This capacitance can be derived using a similar procedure.

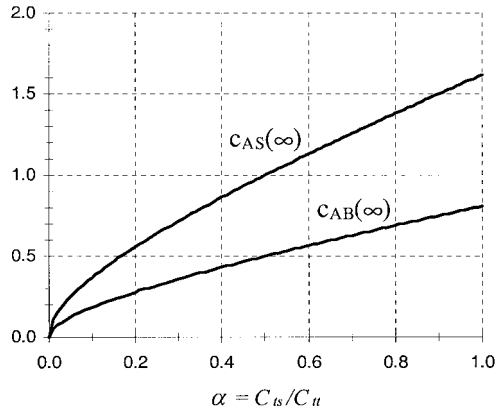

Fig. 8. Normalized capacitances for an infinite number of turns as a function of the capacitance ratio α.

Starting from $C_{AS}(1) = C_{ts}$, we obtain

$$C_{AS}(n) = \frac{C_{AS}(n-1)\cdot C_{tt}}{C_{AS}(n-1) + C_{tt}} + C_{ts}, \qquad \text{for } n > 1. \tag{7}$$

From (7), we can normalize $C_{AS}(n)$ with respect to C_{tt} and introduce the ratio α to obtain

$$c_{AS}(n) = \frac{C_{AS}(n)}{C_{tt}} = \frac{1}{1 + C_{tt}/C_{AS}(n-1)} + \alpha. \tag{8}$$

Fig. 7 shows that (8) converges to a finite limit for increasing the number of turns n. We found that the expression of such a limit as a function of α is given by

$$c_{AS}(\infty) = \frac{C_{AS}(\infty)}{C_{tt}} = \frac{1}{2}\,(\alpha + \sqrt{\alpha^2 + 4\alpha}). \tag{9}$$

Notice that the limit obtained in (9) is twice the limit given by (6). Equations (6) and (9) are plotted in Fig. 8. In order to obtain the capacitances C_1 and C_2 of the π-circuit model of Fig. 5, we must impose that the capacitances between terminals and between each terminal and the shield have the same values of the corresponding capacitances of the circuit

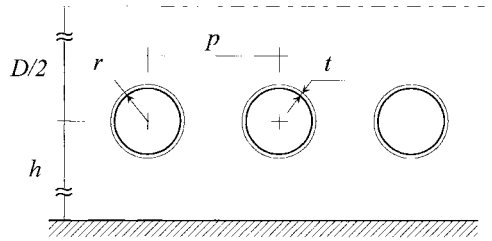

Fig. 9. Cross-sectional view of a coil and shield.

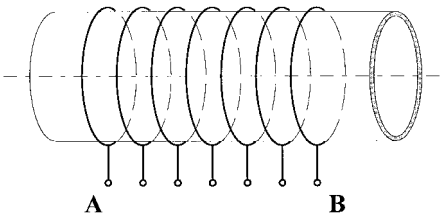

Fig. 10. Wire loop arrangement for stray capacitance measurements.

shown in Fig. 4. Namely, we impose the following conditions:

$$C_{AB} = C_1 + \frac{C_2}{2}$$
$$C_{AS} = C_2 + \frac{C_1 \cdot C_2}{C_1 + C_2}. \tag{10}$$

Hence, we obtain

$$C_1 = C_{AB} - \frac{C_{AB} \cdot C_{AS}}{4C_{AB} - C_{AS}}$$
$$C_2 = 2\frac{C_{AB} \cdot C_{AS}}{4C_{AB} - C_{AS}} \tag{11}$$

where C_{AB} and C_{AS} are given by (4) and (7), respectively.

C. Calculation of Turn-to-Turn and Turn-to-Shield Capacitances

The cross-sectional view of uniformly wound wires of circular cross sections with a shield is shown in Fig. 9. We assume that the capacitance between two adjacent turns C_{tt} can be calculated from the formula for the capacitance per unit length of two infinitely long straight parallel conductors placed in a homogeneous medium. Hence, for this purpose, the turn curvature is neglected. Under these assumptions and when the thickness t of the insulating coating is small compared with the air-gap distance $g = (p - 2r)$, an analytical expression for the turn-to-turn capacitance C_{tt} can be derived for wires of circular cross section [14] as

$$C_{tt} = \frac{\pi^2 D\epsilon_o}{\ln(p/2r + \sqrt{(p/2r)^2 - 1}\,)}, \qquad \text{for } t \ll p - 2r \tag{12}$$

where D is the turn diameter, p is the winding pitch (i.e., the distance between the centerlines of two adjacent turns), and r is the wire radius.

When the thickness t of an insulating coating of relative permittivity ϵ_r is comparable with the air gap, the following expression is derived in the Appendix assuming a radial field in the insulating coating:

$$C_{tt} = \frac{\pi^2 D\epsilon_o}{\ln(F + \sqrt{F^2 - (1 + t/r)^{2/\epsilon_r}}\,)} \tag{13}$$

where

$$F = \frac{p/2r}{(1 + t/r)^{1-1/\epsilon_r}}. \tag{14}$$

We can evaluate the turn-to-shield capacitances of the structure by neglecting the curvature of both the turns and the shield. We also neglect the contribution of the insulating coating. Under these assumptions, we can calculate the turn-to-shield capacitance C_{ts} from the formula of the capacitance per unit length between an infinitely long straight conductor and a parallel conducting plane given by [14]

$$C_{ts} = \frac{2\pi^2 D\epsilon_o}{\ln(h/r + \sqrt{(h/r)^2 - 1}\,)} \tag{15}$$

where h is the distance between the shield and the coil winding.

It should be noted that, in the calculation of turn-to-turn and turn-to-shield capacitances by (12) and (15), respectively, their mutual influence is neglected. The interaction between the corresponding capacitive effects is taken into account introducing these stray capacitances in the equivalent circuit of Fig. 4.

III. Comparison of Numerical and Experimental Results

In order to validate the proposed method, single-wire rings without insulating coating were considered. These rings of circular cross section were arranged as the turns of an HF coil. The arrangement for $n = 7$ is shown in Fig. 10. Notice that Fig. 10 reflects the inductor behavior represented by the equivalent circuit model of Fig. 4, in which the autotransformer action of the winding is not significant.

Three sets of rings were used for the measurements. The geometrical parameters of the rings are given in Table I. For each set, different pitches were considered. The measurements were carried out by means of a HP 4192A LF Impedance Analyzer. Measured and calculated values for the turn-to-turn capacitance C_{tt} are given in Table I. As expected, no significant difference was found for measured capacitances in the frequency range between 10 kHz–1 MHz. Good agreement between the measured and calculated values of the turn-to-turn capacitance C_{tt} indicates that the analytical formula (12) is sufficiently accurate when $D/2r > 5$. Fig. 11 shows the measured overall stray capacitance C_{AB} for coils of type 1 having four different winding pitches as a function of the number of turns. Since a shield was not present, the corresponding calculated values were obtained from (1) when C_t is assumed to be equal to C_{tt} or from (2)–(4), when $C_{ts} = 0$. Because turn-to-turn capacitances between nonadjacent turns have been neglected in the calculations, the measured overall capacitances were larger than the calculated ones given by (1). For a coil with $n = 10$, the relative error increased from 12% to 23% when the winding pitch-to-wire diameter ratio $p/2r$ increased from 1.61 to 2.57. These results

TABLE I
GEOMETRICAL PARAMETERS OF RINGS

Coil No.	Ring Diameter D [mm]	Wire Radius r [mm]	Pitch p [mm]	Meas. C_{tt} [pF]	Calc. C_{tt} [pF]
1a	47.2	3.25	6.90	11.7	11.82
1b	47.2	3.25	7.32	8.2	8.30
1c	47.2	3.25	9.00	4.7	4.85
2a	36.0	2.70	5.70	9.4	9.48
2b	36.0	2.70	5.98	6.8	6.85
2c	36.0	2.70	7.33	3.8	3.83
3a	26.9	2.12	4.59	5.8	5.82
3b	26.9	2.12	5.05	3.8	3.86
3c	26.9	2.12	6.57	2.3	2.34

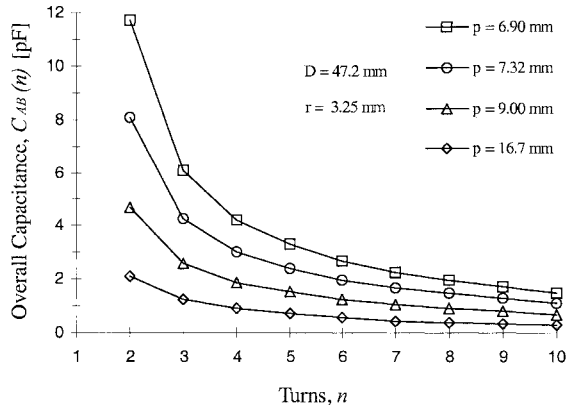

Fig. 11. Measured capacitances for different values of the winding pitch.

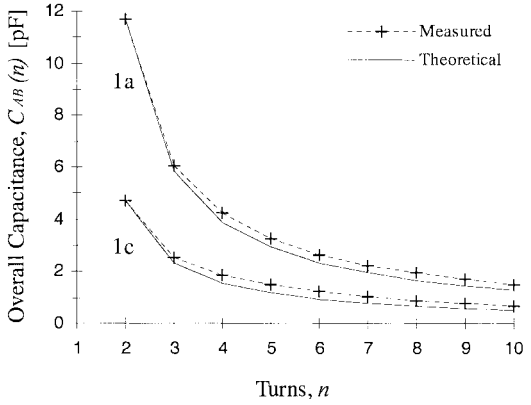

Fig. 12. Measured and calculated capacitances as a function of the number of turns for the coils *1a* and *1c*.

confirm that, as a rule of thumb, the assumption of neglecting capacitances between nonadjacent turns is reasonable when the ratio $p/2r$ is less or equal to two.

Figs. 12–14 show the measured and calculated capacitances for the coils *a* and *c* of the types 1–3, respectively. Coils *1b*, *2b*, and *3b* having values within coils *a* and *c* of all types have been omitted for the sake of readability. The experimental results prove that the proposed HF equivalent circuit of Fig. 4 is sufficiently accurate and the percentage of error increases for increasing values of the winding pitch-to-wire-diameter ratio.

In order to verify the correctness of the measuring procedure adopted, a test inductor consisting of $n = 16$ turns with wire of radius $r = 5$ mm, turn diameter $D = 326$ mm, and pitch $p = 10.2$ mm was built. The coil inductance calculated using the method presented in [12] is $L_c = 82.4$ μH, and the measured inductance was $L_m = 82.3$ μH at $f = 10$ kHz. The capacitance between two adjacent turns calculated from (12) is $C_{tt} = 143$ pF. Consequently, the calculated overall stray capacitance is $C_{AB} = 9.5$ pF. The first self-resonant frequency was measured to be $f_{0m} = 5.1$ MHz. Hence, the overall stray capacitance $C_m = 11.8$ pF is derived. The discrepancy between the values of C_{AB} and C_m is about 19%. However, the calculated value does not take into account the electric effects of plastic spacers we put all around the coil to maintain approximately a constant distance between the relatively large turns of such a coil. These plastic spacers, present for a 10% of the total turn length, can be primarily responsible for the higher capacitance measured in the experiment. From this test, it can

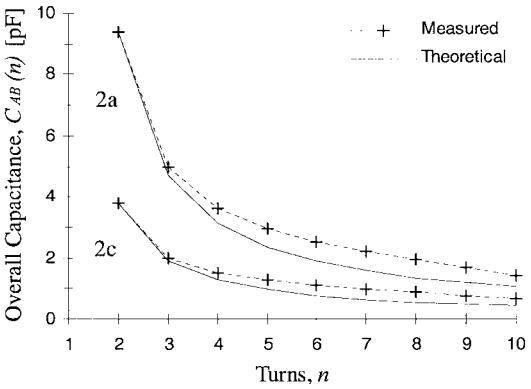

Fig. 13. Measured and calculated capacitances as a function of the number of turns for the coils *2a* and *2c*.

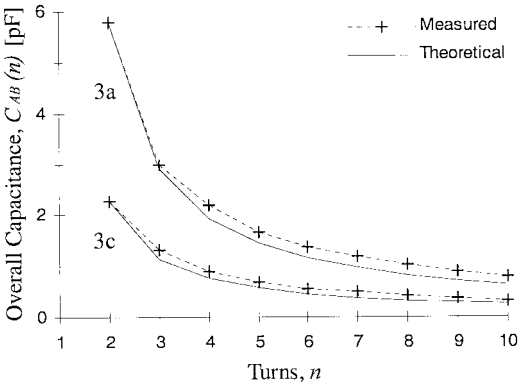

Fig. 14. Measured and calculated capacitances as a function of the number of turns for the coils *3a* and *3c*.

be seen that the procedure we adopted in previous experiments by measuring the capacitance between rings is quite reasonable for the type of coils examined.

IV. Conclusions

The overall stray capacitance of single-layer solenoid air-core inductors was derived starting from an equivalent circuit, the main and parasitic parameters of which are related to every turn or pair of turns of the coil. From this circuit, two simplified models of inductors are derived. The former includes the resistance and the series equivalent inductance of each turn and the turn-to-turn capacitances between adjacent turns. This model is valid when there is no shield or the influence of the shield on the capacitance is negligible. The latter model consists of a capacitive network with turn-to-turn and turn-to-shield capacitances and is valid above the self-resonant frequency. An analytical approach to determine the turn-to-turn and turn-to-shield capacitances has been presented. Various structures of inductors were built and tested. Good agreement between calculated and measured results proves that the proposed method for predicting stray capacitances is reliable and suitable for the design and analysis of inductors in a high-frequency range.

Appendix

In order to derive (13) of Section II-C, we consider the equivalent capacitance of the series combination of the capacitances related to the insulating coatings and the capacitance related to the air gap between turns. Using the cylindrical capacitor formula, we obtain the per-unit length capacitance C_c related to an insulating coating

$$C_c = \frac{2\pi\epsilon}{\ln(1+t/r)}. \tag{A1}$$

The per-unit length capacitance C_g related to the air gap between adjacent turns can be calculated from (12) replacing the wire radius r with the external coating radius $(r+t)$

$$C_g = \frac{\pi\epsilon_o}{\ln\left(\dfrac{p/2r}{1+t/r} + \sqrt{\left(\dfrac{p/2r}{1+t/r}\right)^2 - 1}\right)}. \tag{A2}$$

Using (A1) and (A2), one obtains the equivalent capacitance per-unit length

$$\begin{aligned} C_{\text{eq}} &= \frac{C_c C_g}{C_c + 2C_g} \\ &= \frac{\pi\epsilon \cdot \epsilon_o}{\ln[(1+t/r)^{\epsilon_o} \cdot (B + \sqrt{B^2-1}\,)^{\epsilon}]} \end{aligned} \tag{A3}$$

where $B = (p/2r)/(1+t/r)$.

We can write the denominator of (A3) in the form

$$\begin{aligned} &\ln[(1+t/r)^{\epsilon_o} \cdot (B + \sqrt{B^2-1}\,)^{\epsilon}] \\ &\qquad = \epsilon \cdot \ln[(1+t/r)^{\epsilon_o/\epsilon} \cdot (B + \sqrt{B^2-1}\,)]. \end{aligned} \tag{A4}$$

After algebraic manipulations and introducing the turn length πD, one obtains (13) of Section II-C from (A3) and (A4).

References

[1] P. L. Dowell, "Effects of eddy currents in transformer windings," *Proc. Inst. Elect. Eng.*, vol. 113, no. 8, pp. 1387–1394, Aug. 1966.
[2] W. M. Flanagan, *Handbook of Transformer Applications*. New York: McGraw-Hill, 1986.
[3] N. R. Grossner, *Transformers for Electronic Circuits*, 2nd ed. New York: McGraw-Hill, 1983.
[4] W. T. Duerdoth, "Equivalent capacitances of transformer windings," *Wireless Eng.*, vol. 23, pp. 161–168, June 1946.
[5] D. Maurice and R. H. Minns, "Very-wide-band radio-frequency transformers—Part I," *Wireless Eng.*, vol. 24, pp. 168–177, June 1947.
[6] ———, "Very-wide-band radio-frequency transformers—Part II," *Wireless Eng.*, vol. 24, pp. 209–216, July 1947.
[7] K. A. Macfadian, *Small Transformers and Inductors*. London, U.K., Chapman & Hall, 1953.
[8] H. Zuhrt, "Einfache Näherungsformeln für die Eigenkapazität Mehrlagiger-Spulen," *Elektrotech. Z.*, vol. 55, pp. 662–671, 1934.
[9] R. G. Medhurst, "H. F. resistance and self-capacitance of single-layer solenoids—Part I," *Wireless Eng.*, vol. 24, pp. 35–43, Feb. 1947.
[10] ———, "H. F. resistance and self-capacitance of single-layer solenoids—Part II," *Wireless Eng.*, vol. 24, pp. 80–92, Mar. 1947.
[11] A. Massarini and M. K. Kazimierczuk, "Modeling the parasitic capacitance of inductors," in *Proc. Capacitor and Resistor Technology Symp.* (CARTS'96), New Orleans, LA, Mar. 1996, pp. 78–85.
[12] A. Massarini, M. K. Kazimierczuk, and G. Grandi, "Lumped parameter models for single- and multiple-layer inductors," in *Proc. PESC'96*, Baveno, Italy, June 1996, pp. 295–301.
[13] M. Kostenko and L. Piotrovsky, *Electrical Machines*, vol. 1. Moscow, U.S.S.R.: Mir, 1968.
[14] A. A. Zaky and R. Hawley, *Fundamentals of Electromagnetic Field Theory*. London, U.K.: Harrap, 1974.

Gabriele Grandi was born in Bologna, Italy, in 1965. He received the M.Sc. (*cum laude*) and the Ph.D. degrees from the Faculty of Engineering, University of Bologna, Bologna, Italy, in 1990 and 1994, respectively, both in electrical engineering.

Since 1995, he has been an Assistant Professor (Research Associate) in the Department of Electrical Engineering, University of Bologna. His research interests are modeling, simulation, and design of electronic power converters, in particular, power conditioning systems. He is currently studying EMC problems related to electric power apparatus and systems, mainly, switching converters and circuit models of HF components.

Marian K. Kazimierczuk (M'91–SM'91) received the M.S., Ph.D., and D.Sci. degrees in electronics engineering from the Department of Electronics, Technical University of Warsaw, Warsaw, Poland, in 1971, 1978, and 1984, respectively.

He was a Teaching and Research Assistant from 1972 to 1978 and Assistant Professor from 1978 to 1984 in the Department of Electronics, Institute of Radio Electronics, Technical University of Warsaw. In 1984, he was a Project Engineer with Design Automation, Inc., Lexington, MA. During 1984–1985, he was a Visiting Professor with the Department of Electrical Engineering, Virginia Polytechnic Institute and State University, Blacksburg. Since 1985, he has been with the Department of Electrical Engineering, Wright State University, Dayton, OH, where he is currently a Professor. His research interests are high-frequency high-efficiency switching-mode tuned power amplifiers, resonant and PWM dc/dc power converters, dc/ac inverters, high-frequency rectifiers, electronic ballasts, magnetics, power semiconductor devices, and applied controls, He is the coauthor of *Resonant Power Converters* (New York: Wiley, 1995). He has published over 200 technical papers, more than 70 of which have appeared in IEEE Transactions and Journals. He serves as an Associate Editor of the *Journal of Circuits, Systems, and Computers*.

Dr. Kazimierczuk received the IEEE Harrell V. Noble Award in 1991 for his contributions to the fields of aerospace, industrial, and power electronics. He is also a recipient of the 1991 Presidential Award for Faculty Excellence in Research, the 1993 College Teaching Award, the 1995 Presidential Award for Outstanding Faculty Member, and Brage Golding Distinguished Professor of Research Award from Wright State University. He has been an Associate Editor of the IEEE TRANSACTIONS ON CIRCUITS AND SYSTEMS PART I. He was a member of the Superconductivity Committee of the IEEE Power Electronics Society. He is a member of Tau Beta Pi.

Antonio Massarini received the Laurea degree (*cum laude*) in nuclear engineering and the Ph.D. degree in electrical engineering from the University of Bologna, Bologna, Italy, in 1987 and 1992, respectively.

Since 1993, he has been a Teaching and Research Assistant with the Faculty of Engineering, Department of Engineering Sciences, University of Modena and Reggio Emilia, Modena, Italy. He also cooperates with the Electrical Engineering Department of the University of Bologna, and was a Visiting Professor with the Department of Electrical Engineering, Wright State University, Dayton, OH. His research interests include MHD flow simulation, switched network simulation, magnetics, numerical methods for circuit analysis and design, and switching power converter simulation and design.

Ugo Reggiani (M'92) received the Laurea degree (*cum laude*) in electrical engineering from the University of Bologna, Bologna, Italy, in 1969.

He was appointed as an Assistant with the Faculty of Engineering, University of Bologna, in 1972, and became an Assistant Professor in 1974 and a Full Professor of electrotechnics in 1980. He is also currently Head of the Department of Electrical Engineering. His main research interests concern electromagnetic field theory, electrical machines and drives, electromagnetic compatibility, circuit analysis, and modeling of switched networks.

Prof. Reggiani is a member of the Italian Electrotechnical and Electronic Association (AEI) and the IEEE Industry Applications Society.